

Evolution of lithiation thermodynamics with the graphitization of carbons

Y. Reynier^a, R. Yazami^{a,*}, B. Fultz^a, I. Barsukov^b

^a Caltech CNRS International Laboratory on Materials for Electrochemical Energetics, Division of Engineering and Applied Science, California Institute of Technology, MC 138-78, Pasadena, CA 91125, USA

^b Superior Graphite Co., 10 S. Riverside Plaza, Chicago, IL 60606, USA

Available online 17 November 2006

Abstract

Instrumentation was developed to study the thermodynamics of lithium intercalation in cokes that were heat-treated at different temperatures. The method measures the open circuit voltages of electrochemical cells as a function of temperature, and obtains the entropy and enthalpy of the lithiation reaction. X-ray diffractometry and Raman spectroscopy were used to determine the structure of the carbon materials after heat treatment. The effect of the degree of graphitization on the entropy and enthalpy of lithium intercalation was thereby determined. A model is proposed to correlate the degree of graphitization to entropy profiles. It is shown that graphs of entropy versus open circuit voltage for different states of charge give quantitative information on graphitization, making them useful for the structural characterization of partially-graphitized carbons.

© 2006 Elsevier B.V. All rights reserved.

Keywords: Carbon; Graphite; Lithium; Thermodynamics; Entropy

1. Introduction

Carbonaceous materials, especially graphite, are the active materials in most anodes of commercial rechargeable lithium batteries. The crystallinity and defect structures in these materials affect the lithium intercalation reaction, altering the cyclability, stability, and rate capability of the battery. In the present work, a series of cokes subjected to various heat treatment temperatures were prepared for a systematic study of the effect of graphitization on the thermodynamics of lithium intercalation.

In previous work [1], we showed that curves of the entropy and enthalpy of the lithiation reaction vary greatly between graphite and disordered carbons. This is perhaps expected because the structures of these two carbonaceous materials are very different. The long-range order of graphite accommodates lithium up to LiC_6 , and the lithiation reaction occurs in stages with the formation of different orderings of lithium atoms. The entropy curves consequently show several distinct regions with plateaus, typical of first order phase transitions. On the other hand, the mechanism of lithium insertion into carbonaceous materials is not well understood [2].

Our previous work showed that measurements of the entropy and enthalpy differed between graphite materials subjected to

different processings, and some sources of entropy could be identified in the curves of entropy versus state of lithiation. The present study was focused on carbonaceous materials with low and intermediate degrees of graphitization. It is shown that graphs of entropy versus open circuit voltage at different states of charge can be used to deduce the degree of graphitization of the carbonaceous materials. These thermodynamics results are at least as sensitive to structural changes in partially-graphitized carbons as are X-ray diffractometry and Raman spectrometry.

2. Experimental

A series of coke samples was provided by Superior Graphite Co. (Chicago, IL, USA). Along with the precursor that had undergone no heat treatment, materials were obtained after heat treatments at 900, 1100, 2200 and 2600 °C under an argon atmosphere. The average particle size was 30 μm. A petroleum coke heat-treated at 1700 °C (provided by Carbone Lorraine, Aubervillier, France) was also studied. Composite electrodes were made by casting a slurry composed of 85% active material and 15% PVDF dissolved in acetone. No electronic binder was used because it could influence the thermodynamic measurements.

Coin cells of the CR2016 design were assembled in an argon-filled glove box. The electrolyte consisted of a molar solution of LiPF_6 in an EC:DMC (vol. 1:1) solvent mixture. The cells

* Corresponding author.

E-mail address: yazami@caltech.edu (R. Yazami).

were first cycled five times with a rate of $C/10$ between 5 mV and 1.5 V versus Li to achieve a stable capacity. An automated thermodynamic measurement system (TMS) was then used to measure open circuit voltage versus temperature on pairs of cells with the same carbon material. A precision voltmeter (Agilent 34970, 10 μ V resolution) measured an open circuit voltage while the cells were cooled with a Peltier plate controlled by a power supply. Six temperature steps were made with a 2 °C difference between each. Twenty minutes of equilibration was allowed for each step, which was confirmed to be enough time for the potential to stabilize. The temperature was measured with two RTD elements accurate to 0.1 °C, one attached to the Peltier plate and the other to the test cell. Owing to the reasonable thickness of the cell and adequate thermal conductivities, the temperature of both RTD elements became equal a few minutes after each step. After each six-step potential measurement, the composition was changed by a galvanostatic charge or discharge, and a rest time of 4 or 8 h was used before the next temperature cycle. The temperature dependence of the open circuit voltage was then reduced to the entropy and enthalpy of lithium intercalation at different states of charge.

Considering the high resolution of the instrumentation, a temperature range of 10 °C is sufficient to get accurate data while minimizing the chance of a temperature induced phase transition or a large change in electrochemical kinetics, for example. Going below room temperature minimizes self-discharge during the experiment, and the remaining voltage drift is automatically subtracted by measuring the voltage difference between the start of the experiment and 2 h after termination. The lithium composition, x , is determined by using the current passed through the cell and the active mass to calculate the capacity, and then comparing it to the theoretical capacity of graphite (372 mAh g^{-1}).

X-ray diffraction (XRD) patterns were acquired with a Philips X'Pert diffractometer using the Cu $K\alpha$ X-rays. Ten percent of silicon powder was added to each sample to provide an internal reference and give an accurate peak position measurements. Raman spectra were acquired on a Renishaw micro Raman spectrometer using the 514.5 nm radiation of an argon ion laser. The spectral resolution was 1 cm^{-1} .

3. Results

X-ray diffraction patterns from the different materials are presented in Fig. 1. With increasing heat treatment temperature, there is a sharpening of the graphite 002 diffraction peak at about $2\theta = 26^\circ$. For temperatures of 2200 °C and higher, the 004 peak is visible at $2\theta = 54^\circ$. The presence of the 004 peak is indicative of higher crystallinity.

The materials heat-treated at the three lowest temperatures cannot be distinguished from their XRD patterns alone, as expected since graphitization treatments are not so effective for temperatures below 1000 °C [3]. The 101 diffraction peak of the rhombohedral phase can be seen near 45° , indicating that the crystalline domains of the cokes consisted of a mixture of hexagonal and rhombohedral graphite. Noteworthy is the shape of the 002 peak for the materials heat-treated at low temperatures, where a sharp peak at $2\theta = 26.4^\circ$ is present next to a broader peak

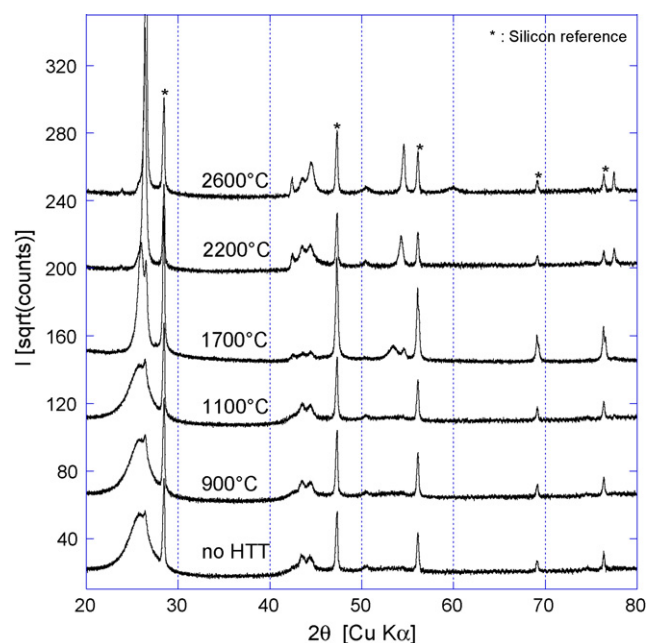


Fig. 1. XRD pattern of the coke samples heat-treated at different temperatures, with an internal silicon reference (labeled *).

at 25.7° . The sharp peak shows that well-graphitized domains are present even in these samples with low temperature heat treatments.

The degree of graphitization G was determined from the d -spacing of the 002 peaks, using the following formula [4]:

$$G = \frac{3.461 - d_{002}}{3.461 - 3.352} \quad (1)$$

where 3.461 Å is the d -spacing for a fully turbostratic disordered material and 3.352 Å is the d -spacing of highly oriented pyrolytic graphite. The parameter G decreases with the proportion of turbostratic disorder, and is a measure of the degree of graphitization. The XRD results are summarized in Table 1.

Some Raman spectra of the samples are shown in Fig. 2. Raman spectra can provide information on the disorder in the 'a'

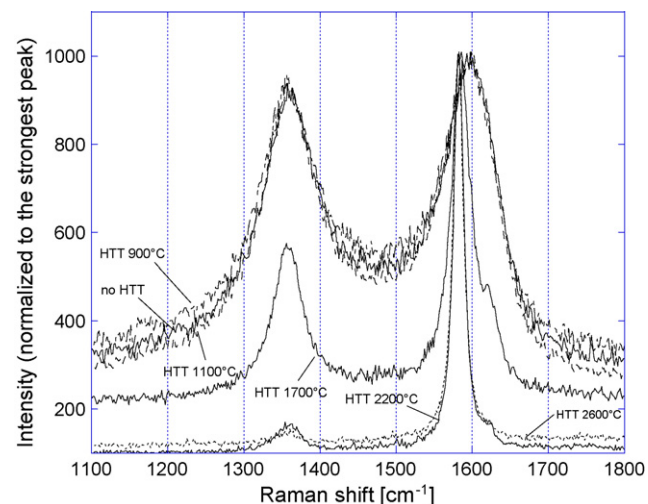


Fig. 2. Raman spectra for all samples.

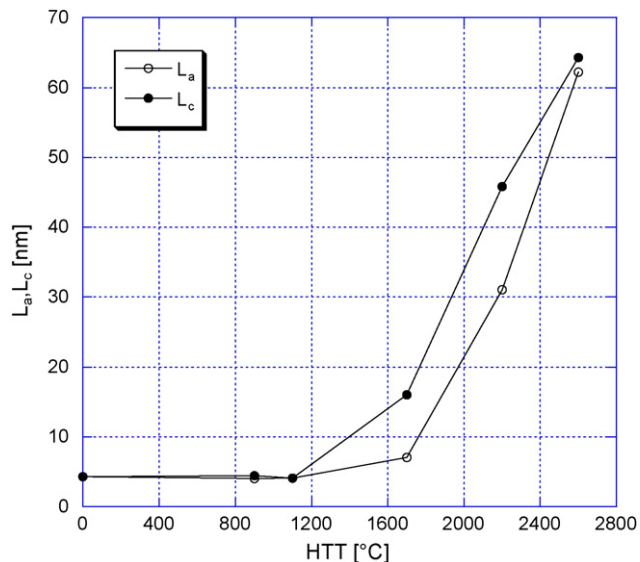


Fig. 3. Crystal coherence lengths as a function of heat treatment temperature based on Raman spectroscopy, L_a , and L_c from XRD patterns.

direction from the intensity ratio of the D band peak (A_{1g} breathing mode) at 1355 cm^{-1} and the G band peak (E_{2g2} stretching mode) at 1590 cm^{-1} . The D band is caused by vibrations that occur only when the graphene planes are small, and indicate disorder in the carbonaceous material. The crystallite size in the ‘a’ direction, L_a , can be estimated with the equation suggested by Tuinstra and Koenig [5]:

$$L_a = \frac{4.3}{R} \quad (2)$$

with R defined as the ratio of the integrated intensity of the D and G peaks.

With increasing temperature of heat treatments, there is a decrease in intensity of the D band peak, and the G band peak becomes sharper, while shifting downward [6]. The calculated L_a versus temperature is presented in Fig. 3, and is compared to the L_c values obtained by XRD. The values found for L_a are similar to those determined for L_c from X-ray diffractometry, and confirm the increase in size of crystallites for heat treatments above 1500 °C . Below this temperature, L_a and L_c both have a value of about 4 nm. The size of the crystalline domains increases rapidly with heat treatment temperature, reaching about 65 nm at 2600 °C . X-ray lineshape analysis is only qualitative after crystallite sizes exceed 40 nm, however.

Fig. 4 shows the entropy profile of the precursor material with no heat treatment, and the open circuit voltage (OCV) curve for the same material. These data were recorded during charging of the cell (increasing voltage), using 8 h rest before each temperature cycle. Charging was performed at a $C/20$ rate. The OCV curve has a shape typical of samples with lower temperatures of heat treatments: it decreases steadily with concentration, and the potential is high compared to graphite, exceeding 1 V versus Li^+/Li , and decreases below 0.2 V only at the end of lithium insertion. The entropy curve has several visible features. After a sharp drop for compositions below $x=0.1$, it increases and

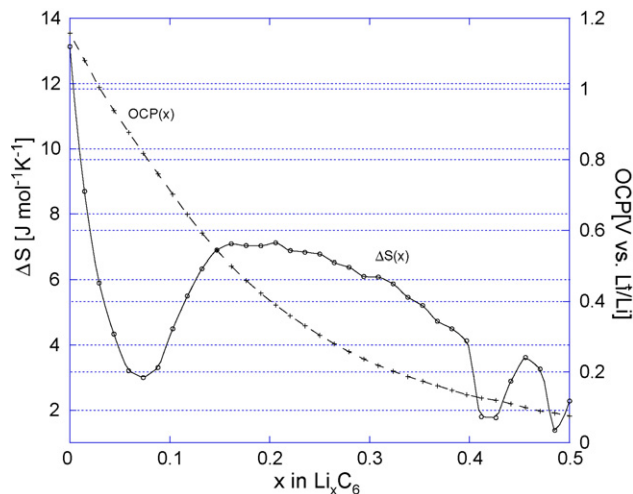


Fig. 4. Entropy of lithium intercalation into coke with no heat treatment and corresponding OCV during charge (delithiation).

makes a plateau between $x=0.2$ and 0.4 . It then decreases to $1\text{ J mol}^{-1}\text{ K}^{-1}$, and finally increases at the very end of insertion.

The entropy curves for lithiation of the three materials with lower temperature heat treatments are presented in Fig. 5. Profiles for the precursor material, and materials heat-treated at 900 and 1100 °C look similar, apart from the region above $x=0.4$. The capacity of these compounds, about 200 mAh g^{-1} , is low compared to graphite but seems to increase a bit with heat treatment.

For heat treatments at higher temperatures, some typical features of ordered graphite appear in the entropy curve and the OCV curve. Fig. 6 shows the entropy and OCV curves for a coke heat-treated at 1700 °C : the potential first drops, and makes two sloping plateaus, hinting at staging. A plateau is also visible in the entropy for x between about 0.3 and 0.5 after an initial peak around $x=0.05$, and the curve decreases for lithium concentrations up to $x=0.25$.

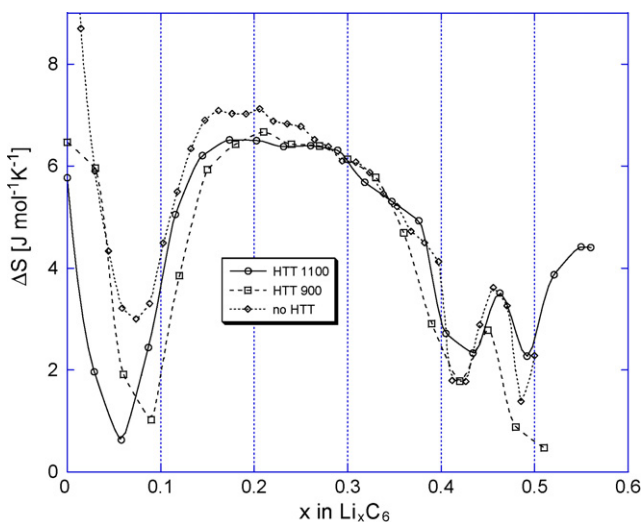


Fig. 5. Comparison of the entropy of lithiation for the samples with low heat treatment temperatures (precursor, 900 and 1100 °C).

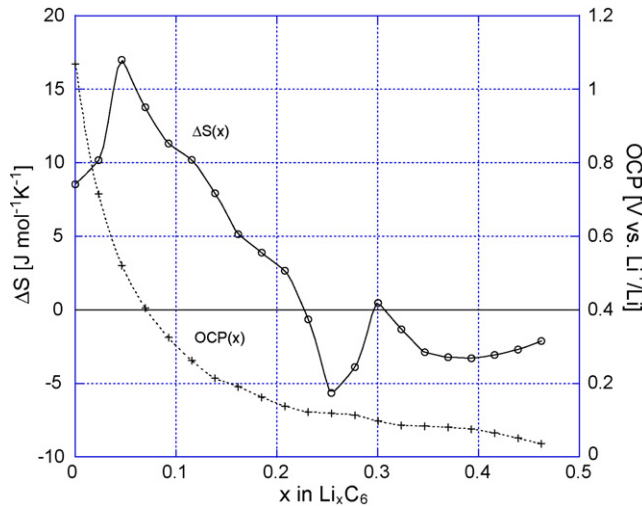


Fig. 6. Entropy of lithiation and OCV of a coke heat-treated at 1700 °C (discharge curve).

With a heat treatment temperature of 2200 °C, the material develops a high degree of crystallographic order. Large graphene planes form and can accommodate lithium in staged reactions. This is seen in Fig. 7 where the sharp entropy step at $x=0.5$ is indicative of the formation of a stage one compound [1]. The capacity is greatly improved by this heat treatment, reaching 275 mAh g⁻¹.

Finally, the coke sample with highest heat treatment temperature of 2600 °C had the highest capacity of our materials, 316 mAh g⁻¹. The OCV and entropy curves (Fig. 8) of this sample are similar to those of natural graphite [7]. The rise of the entropy at the lowest x does not originate from lithium intercalation in the material under study, but rather some other electrochemical couple at high potential above 0.5 V versus Li⁺/Li, perhaps from lithium adsorption on the surfaces of disordered

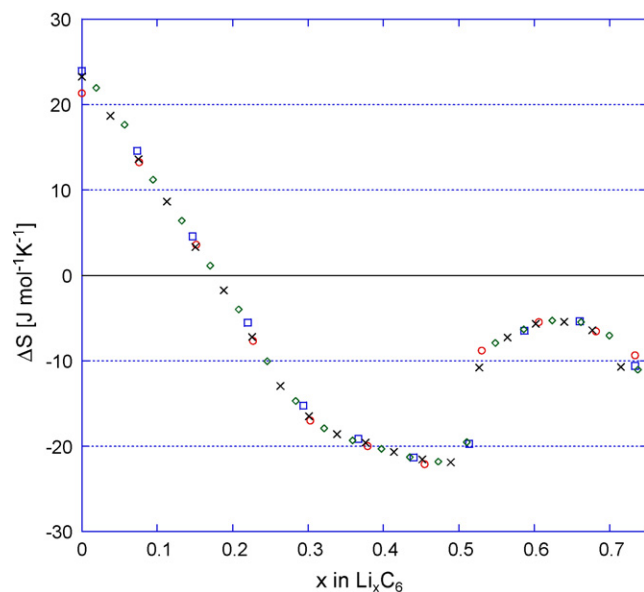


Fig. 7. Entropy of lithiation for the material heat-treated at 2200 °C. Data were averaged from two pairs of cells during discharge to show reproducibility.

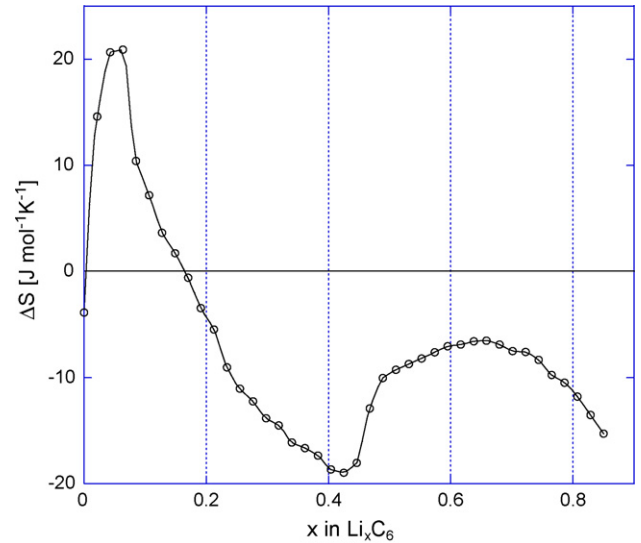


Fig. 8. Entropy of lithiation during discharge of the material heat-treated at 2600 °C.

carbonaceous domains, which may occur prior to intercalation. After the entropy curve decreases rapidly with x below $x=0.1$, it becomes negative and slowly levels off at approximately $x=0.3$. The sharp increase near $x=0.5$ can be seen in the data from the sample heat-treated at 2200 °C. Finally, the entropy curve makes a semi-plateau around -8 J mol⁻¹ K⁻¹ until the full capacity is reached, then begins to fall faster.

The enthalpies of lithiation for the six samples are presented in Fig. 9. For the precursor material, and materials heat-treated at the low temperatures of 900 and 1100 °C, the enthalpy curve mirrors the OCV profiles, because the entropy term in the free energy, TS , is small compared to the average value of enthalpy. This is not the case for the heat treatments at higher temperatures. After a rapid increase, ΔH makes a first peak around $x=0.15$

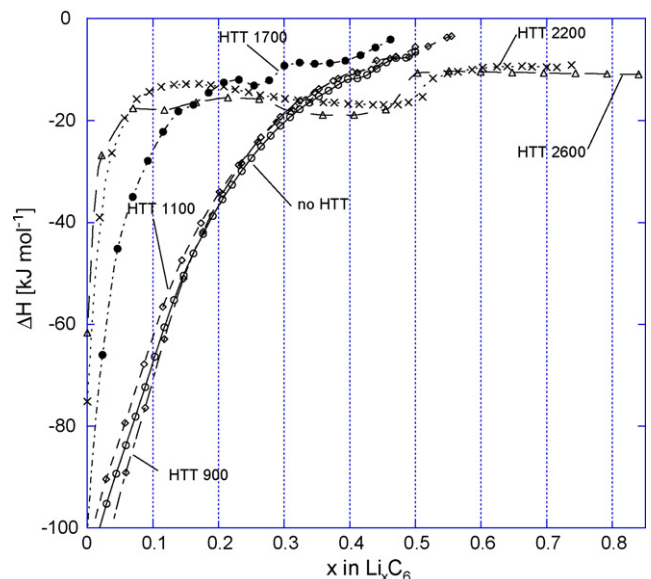


Fig. 9. Enthalpy of lithium intercalation for the five coke samples.

and then shows two plateaus. These plateaus can be related to staging, much as for the entropy profiles.

4. Discussion

4.1. Analysis of the entropy profiles

The enthalpy and entropy curves are greatly influenced by the degree of graphitization, G . Upon a first examination, there seems to be no obvious transition in the shapes of curves for the group of samples with heat treatments at low temperatures and those at high temperatures. This apparent issue is one of data presentation. Comparing curves based on composition, x , does not account for the fact that the inserted sites do not depend on x , but rather on the potential at which the sites become active. Above 0.2 V versus Li^+/Li , the intercalation sites between well-ordered graphene layers are not electrochemically active [8]. This voltage region corresponds to most of the capacity of disordered cokes.

Many theories have been proposed to explain the mode of lithium storage for partially-graphitized carbon materials. Some proposed that lithium could bind covalently with hydrogen at the small graphene plane edges [9], since these materials heat-treated at low temperatures are known to have a high content of hydrogen. Using NMR evidence, Mori et al. [10] postulated the existence of two types of lithium insertion sites, some between graphene planes and others at the surfaces of crystallites, or between them. Another model, called the ‘house of cards’ model, proposes that single-layer graphene fragments are stacked randomly, and lithium is adsorbed on both sides of graphene sheets. Mabuchi et al. [2] proposed a model involving clusters of metallic lithium atoms forming in cavities and pores. In our case, this last possibility seems unlikely, since the clustered lithium atoms would be nearly metallic, and should contribute an extra capacity above $x = 0.5$. They would be inserted at a potential close to 0 V versus Li^+/Li , but this is not observed [11].

Carbons heat-treated at low temperatures below 1100 °C consist of turbostratically disordered graphene planes of different shapes and sizes [12]. For lithium insertion, these materials have a wide range of sites of different energies, resulting in a sloping OCV curve [13]. The change of insertion sites can be seen on potential relaxation curves. The equilibration time after intermittent de-lithiation of a coke with no heat treatment is shorter for potentials below 0.2 V than for potentials between 0.2 and 1 V, indicating differences in kinetic processes.

By applying this interpretation to Fig. 4, it appears that above about $x = 0.33$, the sharp drop in entropy could come from the intercalation of lithium into crystallites of ordered graphite. By analogy with graphite it may be possible that the increase in the entropy curve at larger x may occur after embryos of a lower stage nucleate from the domains of higher staging. The rapid decrease of the entropy curve at small x can be explained by the concentration-dependence of the entropy of mixing. Filling the first available sites in a solid solution causes the entropy of lithiation to change rapidly. From $x = 0.15$ to 0.33, the wide energy distribution of the available sites causes the entropy to be almost zero, since a lithium atom can select only a small number

of equivalently-favored sites. As a result, the partial entropy of insertion should be zero, and the nearly constant value of about $5.5 \text{ J mol}^{-1} \text{ K}^{-1}$ could be explained by the difference of electronic or vibrational entropy between lithium in the metallic anode and the carbonaceous cathode. (Proving this hypothesis would require information on the phonon or electronic entropy of lithiation for disordered carbons.)

At higher temperatures of heat treatment, the region above $x = 0.33$ shows more features. This is consistent with the graphitization process, which should make more graphitic sites available below 0.2 V. It is difficult however to attribute the successive peaks in the $\Delta S(x)$ curves of Fig. 5 to particular staging transitions. The entropy curve for the material heat-treated at 1700 °C is interesting because it constitutes an important link between the behaviors of materials with low and high temperature heat treatments. The electrochemical capacity of the material heat-treated at 1700 °C is low, even compared to the carbons with heat treatments at lower temperatures. The hydrogen content decreases rapidly in the temperature range from 750 to 1500 °C [14], starting at about 10% hydrogen atoms below 750 °C and falling to less than 0.5% for heat treatments above 1500 °C. Fewer sites are consequently available for lithium bonding, but the long-range order of graphite is not yet attained, resulting in a low capacity. The OCV curve for the material heat-treated at 1700 °C (Fig. 6) shows two kinds of behaviors, with a sloping decrease of potential at low x , followed by two plateaus from intercalation between graphene planes as stage 2 and then stage 1 compounds are formed. This mechanism is confirmed in the entropy curve. For materials heat-treated at low temperatures, at low lithium concentrations the entropy curve makes a peak, then decreases and becomes negative when the first plateau appears in the OCV. At x near 0.3, the entropy makes a step increase and reaches a plateau corresponding to stage 1 formation.

The materials heat-treated at 2200 and 2600 °C do not show this dual behavior, but have features very similar to natural graphite. For these materials the only mode of lithiation is lithium intercalation. Their crystallinity is not as good as for natural graphite, however, so the capacity is somewhat lower.

4.2. A two-phase mixture model

We model carbonaceous materials with intermediate degrees of graphitization as a mixture of graphitic and non-graphitic domains. This model suggests a fit of the entropy curves with reference curves from graphitic coke (heat-treated at 2600 °C) and from disordered coke (no heat treatment). However, as pointed out in the previous section, the fit is not a linear combination of the curves based on composition x , but should be based on the OCV, which determines when a lithium insertion site becomes active. For any given potential U , the reference component entropy curves must be combined as:

$$\Delta S(U) = (1 - \alpha)\Delta S_{\text{noHTT}}(U) + \alpha\Delta S_{\text{HTT2600}}(U) \quad (3)$$

where ΔS is the entropy of the material, and α is the fraction of graphitic domains, assuming that the material heat-treated at 2600 °C is fully graphitized.

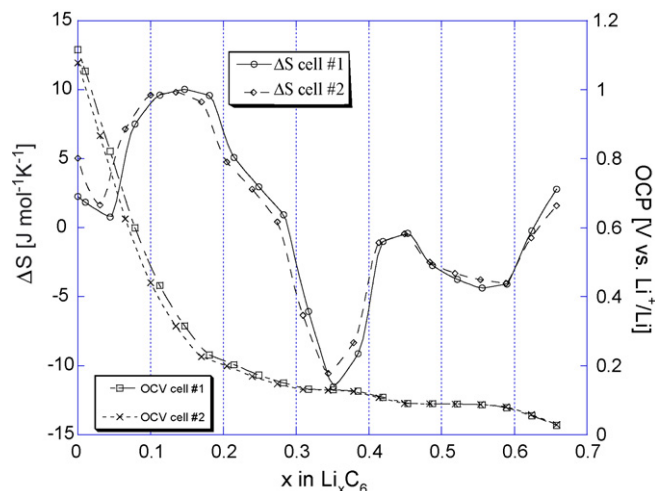


Fig. 10. Evolution of the entropy of intercalation and OCV for a mixture of 50% precursor material and 50% of material heat-treated at 2600 °C (charge curve).

To test this hypothesis, electrodes were prepared using different mixtures of precursor material with no heat treatment and material heat-treated at 2600 °C. First, equal amounts by weight of these two materials were mixed to make an electrode. The measured profiles are shown in Fig. 10. Both entropy and OCV curves look very similar to those of the material heat-treated at 1700 °C (Fig. 6), suggesting that from the standpoint of the lithiation reaction, this material is composed of graphitic and disordered domains.

Another sample was prepared containing a mixture of 25 wt% of precursor material plus 75 wt% of material heat-treated at 2600 °C. As seen in Fig. 11, the capacity increases slightly while the stage 2 to stage 1 plateau of the OCV has a larger range than for the 50/50 sample. It is not surprising to see the curve appear closer to that of the sample heat-treated at 2600 °C because the amount of graphitic material in the electrode was larger. The entropy curves of Figs. 10 and 11 can be compared to the theoretical entropy curve obtained from Eq. (3), with α equal to 0.5 and 0.75, respectively. Fig. 12 compares the entropy of lithium

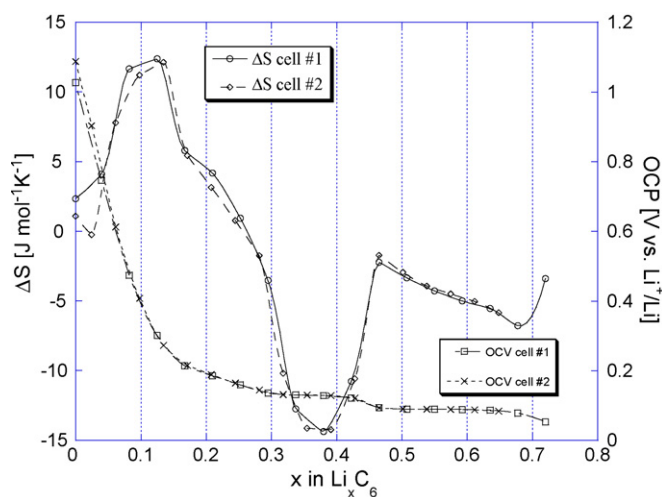


Fig. 11. Evolution of the entropy of intercalation and OCV for a mixture of 25% precursor material and 75% material heat-treated at 2600 °C (charge curve).

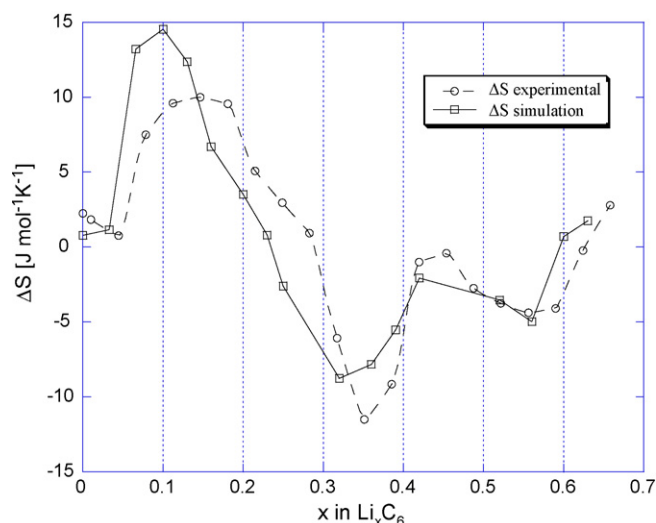


Fig. 12. Entropy of two composite electrodes made with 50% precursor material and 50% material heat-treated at 2600 °C, compared with the calculation of the entropy based on Eq. (3) ($\alpha = 0.50$).

intercalation of a composite electrode made with 50% precursor material and 50% of material heat-treated at 2600 °C, with a calculation based on Eq. (3) using the reference curves. The result from Eq. (3) is in good agreement with experiment, although the entropy is a bit overestimated at low concentrations. The calculation with $\alpha = 0.75$ is shown in Fig. 13, and is compared to electrodes made with 75% of material heat-treated at 2600 °C. There is a very good agreement between experiment and calculation, except again at low concentrations where the entropy is higher for the calculation. These results seem to validate the mixture model of Eq. (3), suggesting that it can be used to determine the fraction of graphitic phase in cokes with different heat treatment temperatures (Table 1).

The entropy curve was then plotted against the OCV curve for each material. These entropy versus OCV plots for the precursor material and for the material heat-treated at 2600 °C were

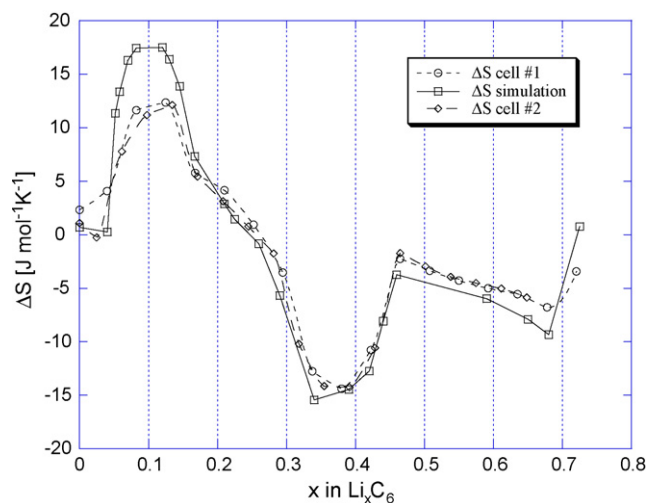


Fig. 13. Entropy of two composite electrodes made with 25% of precursor material and 75% material heat-treated at 2600 °C, compared with the calculation of the entropy based on Eq. (3) ($\alpha = 0.75$).

Table 1
Crystallite size in the *c*-direction based on the 002 peak broadening, and degree of graphitization for materials with different heat treatment temperatures (HTT)

Sample	Full width at half maximum FWHM (2θ)	<i>d</i> -Spacing (Å)	002 peak angle (2θ)	<i>G</i> (%)	<i>L_c</i> (Å)
Coke no HTT	1.97	3.461	25.72	0	43
	0.37	3.372	26.41	82	277
Coke HTT 900 °C	1.93	3.461	25.72	0	44
	0.35	3.372	26.41	82	297
Coke HTT 1100 °C	2.05	3.461	25.72	0	41
	0.33	3.372	26.41	82	320
Coke HTT 1700 °C	0.58	3.428	25.97	30	160
	0.23	3.359	26.51	94	523
Coke HTT 2200 °C	0.25	3.377	26.37	77	458
Coke HTT 2600 °C	0.20	3.361	26.50	92	643

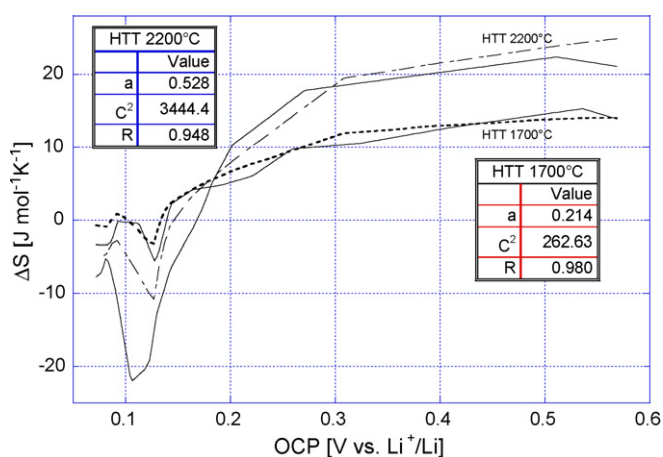


Fig. 14. Parametric plots of entropy curve vs. OCV curve for two samples, heat-treated at 1700 and 2200 °C.

combined following Eq. (3), and α was adjusted to fit similar curves obtained from samples heat-treated at intermediate temperatures. Least squares fits for these entropy versus OCV plots for the cokes heat-treated at 1700 and 2200 °C are shown in Fig. 14. The regression coefficient for the material heat-treated at 1700 °C is good. A value of 21% was obtained for α , close to the 30% graphitization obtained from XRD measurement of the 002 peak position. The degree of graphitization is higher for the material heat-treated at 2200 °C, for which $\alpha = 53\%$, somewhat lower than the value of 77% from the XRD analysis. These values are encouraging and show a good trend, but it must be remembered that even the precursor material used as a reference contained some graphitic domains, thereby introducing an error in α . Likewise the material heat-treated at 2600 °C was used as a reference curve for graphite, but it is not completely graphitized. The use of a coke heat-treated at a higher temperature would improve the accuracy of the result. On the other hand, it might be difficult to find a good reference sample of disordered carbon, since these materials usually have poor electrochemical cyclability.

5. Conclusion

Measurements of open circuit voltage versus temperature were used to study the effect of graphitization on the thermodynamics of lithium intercalation into cokes. Partially graphitized materials show two distinct modes of lithium insertion: cokes subjected to low heat treatment temperatures have lithium insertion into a variety of sites with a wide distribution of energies. As the graphitization improves, lithium atoms intercalate into sites similar to those of graphite. The number of sites of the first type decreases as graphitization proceeds, which results in a mixed behavior for carbonaceous materials that are heat-treated at intermediate temperatures. Experimental results indicate that these carbonaceous materials with intermediate graphitization differ primarily in the amounts of the two types of lithium sites, and the chemical potentials of these sites remain largely unchanged with graphitization. A new method for measuring the degree of graphitization was proposed, based on this model.

References

- [1] Y. Reynier, R. Yazami, B. Fultz, J. Electrochem. Soc. 151 (2004) A422.
- [2] A. Mabuchi, K. Tokumitsu, H. Fujimoto, T. Kasuh, J. Electrochem. Soc. 142 (1995) 1041.
- [3] A. Oberlin, G. Terriere, Carbon 13 (1975) 367.
- [4] J. Mering, J. Maire, J. Chim. Phys. Fr. 57 (1960) 803.
- [5] F. Tuinstra, J.L. Koenig, J. Chem. Phys. 53 (1970) 1126.
- [6] N. Wada, P.J. Gaczi, S.A. Solin, J. Non-Cryst. Solids 35 (1980) 543.
- [7] R. Yazami, Y. Reynier, J. Power Sources 153 (2006) 312.
- [8] H. Kataoka, Y. Saito, O. Omae, J. Suzuki, K. Sekine, T. Kawamura, T. Takamura, Electrochem. Solid-State Lett. 5 (2002) A10.
- [9] P. Papanek, M. Radosavljevic, J.E. Fischer, Chem. Mater. 8 (1996) 1519.
- [10] Y. Mori, T. Iriyama, T. Hashimoto, S. Yamazaki, F. Kawakami, H. Shiroki, T. Yamabe, J. Power Sources 56 (1995) 205.
- [11] M. Letellier, F. Chevallier, F. Béguin, E. Frackowiak, J.-N. Rouzau, J. Phys. Chem. Solids 65 (2004) 245.
- [12] P. Papanek, W.A. Kamitakahara, P. Zhou, J.E. Fischer, J. Phys. Condens. Matter 13 (2001) 8287.
- [13] D.A. Stevens, J.R. Dahn, J. Electrochem. Soc. 148 (2001) A803.
- [14] G. Bathia, R.K. Aggarwal, N. Punjabi, O.P. Bahl, J. Mater. Sci. 32 (1997) 135.